JFE TECHNICAL REPORT
No. 17 (Apr. 2012)

A Seismic Simulation Technology Contributed to Preventing Earthquake Disaster†

UEKI Takuya*1 SHIOZAKI Yoshio*2 KAMURA Hisaya*3

Abstract:

An investigation against the occurrence of a large-scale earthquake predicted to occur in the near future has been carried out in JFE Steel to protect human life, avoid a major disaster to communities in the area and maintain operations. It is important to predict the type of seismic wave the authors encounter in order to prepare reasonable plans for seismic retrofitting of structures and plants. This paper discusses the method estimating the latest strong ground motion using a site amplification factor reflecting local strata inspected by the original boring data and the seismic observation. This method to predict earthquake damages contributes to an effective investment.

1. Introduction

In recent years, the possibility of large-scale earthquakes in the form of a subduction zone earthquake such as a Tonankai-Nankai Earthquake or an epicentral earthquake beneath the Tokyo metropolitan area has been pointed out Central Disaster Management Council (Cabinet Office, Government of Japan) and the Headquarters for Earthquake Research Promotion (Ministry of Education, Culture, Sports, Science and Technology), and seismic retrofitting of buildings and equipment against these large-scale earthquakes has become an important issue in the business continuity plans (BCP) of steel works.

In order to realize reasonable seismic retrofitting, accurate prediction of how expected earthquakes will propagate and arrive is necessary. For this, an accurate assessment of the local strata is critical. On the other hand, multiple steel works exist in different regions, and in addition to plant buildings and production line equipment, these works include a diverse range of other structures such as quay walls, bridges, supporting structures for energy piping, and the like. Since the guidelines and standards to which these structures conform also differ, there is a possibility that differences may also occur in the judgment levels in seismic diagnosis (evaluation of seismic capacity).

Therefore, the authors constructed a rational damage prediction method in order to give proper consideration to the expected earthquakes and ground characteristics in each area and the response characteristics and diagnosis standards for individual structures, while also unifying target seismic strength levels company-wide. This paper describes recent and advanced techniques for predicting strong ground motion (Chapters 2–4) and an earthquake prediction method for structures which is reflected in various design standards (Chapter 5).

2. Expected Earthquakes

In studies of damage prediction, first, it is important to select the large-scale earthquakes which should be assumed. As such earthquakes, the results of a recent survey[1)] of the national government and local governments identified (1) historical earthquakes which are considered to have affected the subject area in the past, (2) earthquakes having an active fault as the hypocenter, and (3) subduction zone earthquakes, among others. The main expected earthquakes are shown in **Fig. 1**. The scenario earthquake which is thought to have the largest impact was selected for each region where steel works are sited, based on a total consideration of the probability of occurrence and scale of these earthquakes, the

† Originally published in *JFE GIHO* No. 27 (Feb. 2011), p. 42–48


*1 Senior Researcher Deputy Manager,
Civil Engineering Res. Dept.,
Steel Res. Lab.,
JFE Steel


*2 Senior Researcher Manager,
Civil Engineering Res. Dept.,
Steel Res. Lab.,
JFE Steel


*3 Dr. Eng.,
General Manager, Civil Engineering Res. Dept.,
Steel Res. Lab.,
JFE Steel

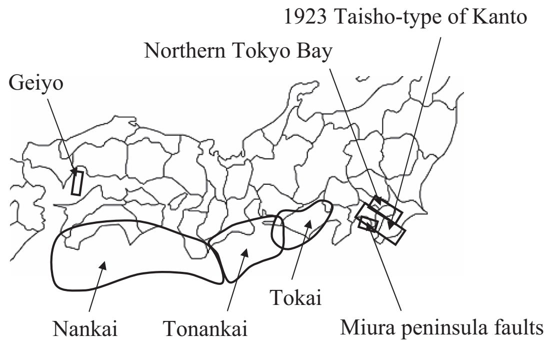

Fig. 1 Main expected earthquakes

importance of the steel works structures, and other factors.

3. Earthquake Damage Prediction Methods

3.1 Outline

The methods generally used to obtain seismic wave for damage prediction were a method using a wave amplified to the expected maximum acceleration level based on the observed seismic wave in the past[2], and a method using a simulated seismic wave which satisfied a target spectrum prepared so as to envelope the mean or maximum values of the response spectra of several earthquakes[3], among others.

However, even among earthquakes with the same intensity level, the seismic wave will differ depending on characteristics of the hypocenter and local strata, and response will differ corresponding to the characteristics of individual structures. Therefore, it is considered necessary to make damage predictions for structures by preparing the ground motion caused by scenario earthquake (scenario ground motion) that reflects these characteristics with good accuracy at the site which requires study.

In response to the 1995 Hyogo-ken Nanbu earthquake, Japan implemented a higher density seismic observation network and various types of exploration to elucidate geological structures. At the same time, rapid progress in research on the fault rupture process and seismic wave path effects has made it possible to predict scenario ground motion with a certain degree of accuracy. A recent example incorporating this knowledge is the "National Seismic Hazard Maps for Japan[1]" published by the Headquarters for Earthquake Research Promotion. Accompanying the revision of the Ports and Harbors Law in May 2006, "Technical Standards and Commentaries for Port and Harbour Facilities in Japan[4]" was revised in July 2007 utilizing the performance-based design approach, and a design method using scenario earthquakes was adopted.

JFE Steel has prepared high accuracy scenario earthquakes by incorporating local ground characteristics,

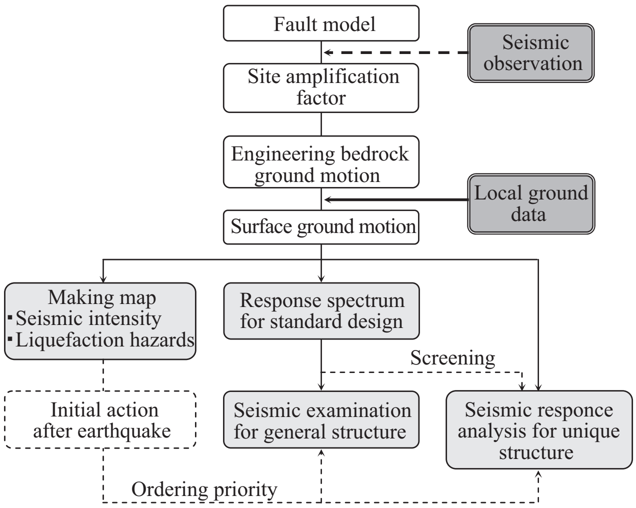

Fig. 2 Flow of earthquake damage prediction method

which properly reflect the company's proprietary ground data and seismic observation data, in recent strong ground motion prediction technology. Based on this, JFE Steel prepared maps contributing to initial action and implemented a seismic capacity evaluation corresponding to the response characteristics of structures, and constructed a framework for efficient and rational estimation of earthquake damage to its steel works. The overall flow of the earthquake damage prediction method is shown in **Fig. 2**.

3.2 Strong Ground Motion Prediction Method

The seismic motion generated at an earthquake source arrives at the seismic bedrock at the site of interest with being influenced by geometrical attenuation (attenuation due to distance) and anelastic attenuation in the ground. Here, the seismic bedrock indicates a stratum where the velocity of the S-wave (secondary or shear wave which arrives after primary wave) is equivalent to 3 000 m/s. It then arrives at the ground surface after repeated amplification corresponding to the ground characteristics of the deep strata (seismic bedrock to engineering bedrock: strata where the S-wave velocity is equivalent of 300–700 m/s) and the shallow strata (engineering bedrock to ground surface).

This means that strong ground motion can be predicted with high accuracy by giving appropriate consideration to (1) the rupture process of the source fault (source effect), (2) the ground motion propagation path from the source fault to the seismic bedrock (path effect), and (3) amplification by strata (sedimentary layers) from the seismic bedrock to the ground surface (site effect).

As the strong motion prediction method used in this paper, the stochastic Green's functions method[5] was adopted because this approach is capable of providing earthquake damage estimation for the entire area

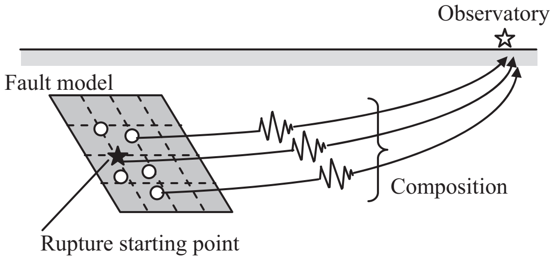

Fig. 3 Concept of the stochastic Green's function method

of a steel works at the ground surface, and the purpose of this research is study of a detailed seismic response analysis for individual superstructures. The stochastic Green's functions method considers empirical site-specific amplification and phase characteristics and has been adopted in design in the port and harbor field.

The stochastic Green's function method is a technique in which the source fault is divided into mesh-like small faults (subfaults), the small seismic waveforms generated from these subfaults are regarded Green's functions. The large earthquake is then composed of chain rupture of the subfaults. **Figure 3** shows a conceptual diagram of the stochastic Green's function method.

Fourier spectrum *O(f)* of the records from the earthquake can be expressed as the product of the source spectrum *S(f)*, the path effect *P(f)*, and the site amplification factor *G(f)*, as shown in Eq. (1).

First, a source (fault) model of the earthquake of interest is prepared. As fault models of expected earthquakes have been proposed by the Central Disaster Management Council and others[6], the use of these models secures consistency with the earthquake damage estimates of the national and local governments. The source spectrum *S(f)* can be evaluated using Eq. (2), which follows the ω^{-2} model, modeling the motion characteristics of earthquake faults simply by frequency domain. The path effect *P(f)* is evaluated by Eq. (3) considering the geometric attenuation and anelastic attenuation of a body wave which expands from the source as a spherical plane. For the site amplification factor *G(f)*, it is possible to use the results obtained by inverse analysis of multiple earthquake records and observation points by Nozu et al.[7], or to obtain a value using the method presented in Section 3.3.

The phase characteristic, which is necessary in preparing ground motion, is extracted from minor and moderate seismic waves at observation points.

$$O(f) = S(f) \cdot P(f) \cdot G(f) \quad \cdots\cdots (1)$$

$$S(f) = R_{\theta\phi} \cdot \mathrm{FS} \cdot \mathrm{PRTITN} \cdot \frac{M_{0e}}{4\pi\rho V_S{}^3} \cdot \frac{(2\pi f)^2}{1 + (f/f_c)^2} \quad \cdots\cdots (2)$$

$$P(f) = \frac{1}{r}\exp(-\pi f r / Q V_S) \quad \cdots\cdots (3)$$

where, $R_{\theta\varphi}$: Radiation coefficient
FS: Amplification due to free surface
PRTITN: Coefficient representing partition of seismic energy into two horizontal components
M_{0e}: Seismic moment of minor earthquake
ρ: Density in the seismic bedrock
V_s: Velocity of S wave in the seismic bedrock
f_c: Corner frequency of minor earthquake ($= 0.66V_s/\sqrt{S_e}$)
S_e: Fault area of minor earthquake
r: Distance from hypocenter
Q: Anelastic attenuation of propagation path

3.3 Prediction of Strong Ground Motion at Engineering Bedrock

The following techniques have been proposed[4] as methods of obtaining the site amplification factor from the seismic bedrock to the engineering bedrock at a littoral location where the site amplification factor is unknown.

Here, $G_K(f)$ and $G(f)$ are the site amplification factors for engineering bedrock and ground surface at the observatory, and $G_P(f)$ and $G'(f)$ are them at the prediction point.

Simplified Method 1: Method of estimating $G_P(f)$ from $G(f)$ using the general relationship (the national average for 124 location) between $G_K(f)$ at the inland zone and $G_P(f)$ at the littoral zone (**Fig. 4** (a)).

Simplified Method 2: Method of estimating $G_P(f)$ by obtaining $G'(f)$ from $G(f)$ using the spectrum ratio of ground motion with simultaneous seismic observations at the known observatory and prediction point, and dividing the $G'(f)$ by the transfer function from the engineering bedrock to the ground surface (Fig. 4(b)).

In preparing the expected intensity map shown in Section 3.5, calculations were made using Simplified Method 1. However, Simplified Method 2 provides

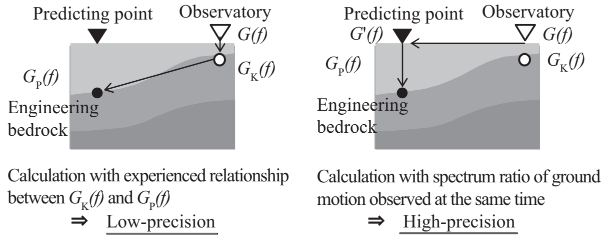

(a) Simplified method 1 (b) Simplified method 2

Fig. 4 Methods of estimating the amplification factor higher accuracy and is used in some cases in detailed analyses of critical structures, based on the results of seismic observation. Simplified Method 2 will be described in detail in Chapter 4.

3.4 Prediction of Strong Ground Motion at Ground Surface

The transfer coefficient from the engineering bedrock to the ground surface is generally obtained by regression analysis from the results of records of past strong motions and is determined separately for each topography/geology. Topographical/geological data have been data-based nationwide in a mesh of approximately 1 km (at present, approximate 250 m mesh) as digital national land information. However, this method is premised on obtaining data at the same level nationwide. While it is effective for macroscopic earthquake damage prediction, it is considered to have low accuracy in damage predictions for more limited areas. Therefore, high accurate site effects were reflected in damage predictions for steel works by collecting and arranging the large volume of boring data which the company had accumulated in the past, and performing ground response analyses for each boring location. As part of that work, the bedrock depth, fine fraction content, etc. were partially complemented by information from the literature and results of subsurface investigations of neighboring areas.

3.5 Expected Intensity Map

It has become possible to prepare local scenario ground motion for each zone in the company's steel works by making strong motion predictions using the procedure described up to this point. Therefore, based on the surface response values (maximum local acceleration, Japan Meteorological Agency seismic intensity, liquefaction potential) at each boring location, expected intensity maps and liquefaction potential maps were prepared for each steel works with a 300 m mesh. These maps are used in assigning priorities to the structures which require study and as basic data for initial action. The image of an expected intensity map is shown in **Fig. 5**.

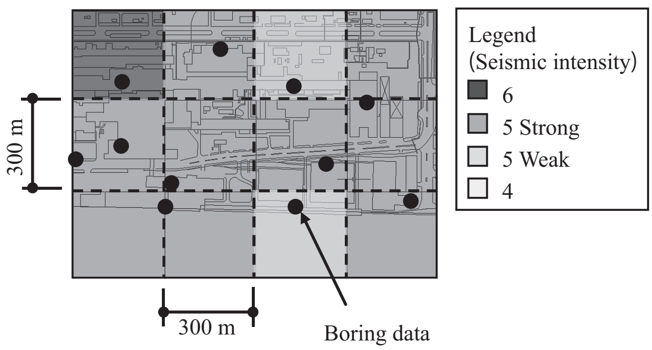

Fig. 5 Image of expected intensity map

4. Improvement of Site Effect Accuracy by Earthquake Observation

4.1 Efforts to Realize Improved Accuracy

In the site amplification factor estimation methods described in Section 3.3, Simplified Method 1 is ultimately based on the national average concept; hence, it is difficult to say that this approach provides an accurate evaluation of the site amplification factor in a specific steel works. In order to improve the accuracy of the site amplification factor by Simplified Method 2, JFE Steel installed state-of-the-art seismographs in 2007 and is conducting ongoing seismic observations in its steel works. Although the number of observations has not yet achieved a sufficient evaluation, this chapter will describe the results of a comparison of the differences in the site effect given by the two methods described previously, using examples of the observation results.

4.2 Example of Seismic Observation

At JFE Steel's West Japan Works Kurashiki District, the following four earthquakes were recorded over a period of approximately 3 years up to the present, simultaneously with earthquakes observed at the K-net[8] observation point (point in Okayama Prefecture nearest to the steel works: OKY012).

(1) March 14, 2008: Earthquake in central Okayama Prefecture (M3.8)
(2) September 3, 2009: Earthquake in southern Kagoshima Prefecture (M6.0)
(3) July 21, 2010: Earthquake in Nara Prefecture (M5.1)
(4) July 23, 2010: Earthquake in western Kochi Prefecture (M4.4)

Although the magnitudes of earthquakes (1) and (4) were small, these were useful events for understanding tendencies. **Figures 6**(a) and **7**(a) show the location of the epicenters and distributions of the maximum acceleration of earthquakes (2) and (3). The acceleration Fourier spectral ratios at West Japan Works Kurashiki District relative to OKY012 are shown in Figs. 6(b) and 7(b). As the spectral ratios of the two earthquakes are roughly in agreement, it can be understood that the response at Kurashiki District is large around 1 Hz.

4.3 Effect on Scenario Ground Motion

Figure 8 shows the site amplification factors $G_P(f)$ estimated by Simplified Method 2 for the earthquakes (1) through (4), together with the results estimated by Simplified Method 1. Eliminating the long period side of earthquake (1), which had a small S/N ratio (ratio of observed signal to noise), all of the site amplification factors estimated by Simplified Method 2 are substantially in agreement. Furthermore, in comparison with

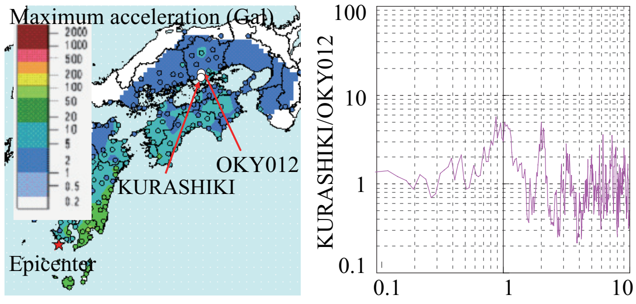

(a) Distribution map of maximum acceleration
(b) Spectral ratio

Fig. 6 Earthquake in southern Kagoshima Prefecture

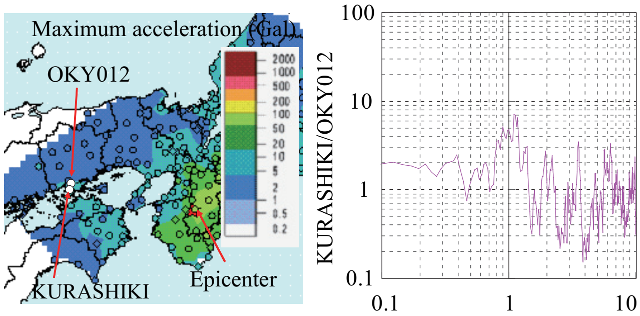

(a) Distribution map of maximum acceleration
(b) Spectral ratio

Fig. 7 Earthquake in Nara Prefecture

Simplified Method 1, a tendency could be seen in which $G_P(f)$ was large on the short period side (i.e., the amplification ratio was high), and small on the long period side.

Here, in order to assess the effect of the differences in these methods on scenario ground motion, scenario ground motions were prepared using the site amplification factors obtained by the respective methods, and a seismic response analysis[9] was carried out for a model steel sheet pile type quay wall[10] (**Fig. 9**) at Port A, which was damaged in the 1983 Nihonkai-Chubu Earthquake. Reproducibility of actual earthquake deformation using this model has been confirmed. **Figure 10** shows the condition of deformation of the quay wall and the distribution of maximum shear strain.

In the analysis results using Simplified Method 2, it can be understood that the amount of earthquake deformation was reduced to approximately 70% in comparison with Simplified Method 1. As the reason for this difference, although the maximum acceleration of the scenario earthquake estimated by Simplified Method 2 was larger, the long period component under 1 Hz was reduced, and this component has a large effect on quay wall deformation.

Since the difference in the site amplification factors have a large effect on scenario ground motions, as illustrated above, a reevaluation using scenario ground motions reflecting the results of seismic observation was carried out for some critical structures.

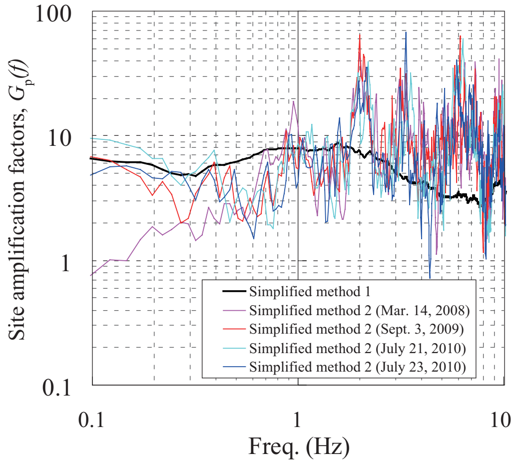

Fig. 8 Comparison of site amplification factors with different method

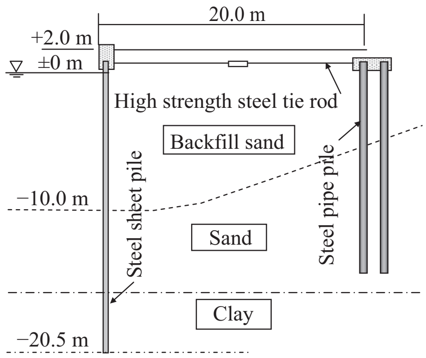

Fig. 9 The sheet pile type quay wall at Port A

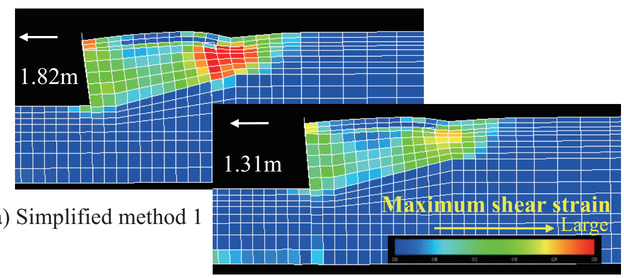

(a) Simplified method 1
(b) Simplified method 2 (Sept. 3, 2009)

Fig. 10 Result of seismic analysis

5. Evaluation of Seismic Capacity of Structures

5.1 Example of Detailed Dynamic Analysis

The chapter describes evaluation of seismic capacity for individual structures using scenario ground motions prepared by the method described above. First, this section will introduce an example of a detailed dynamic analysis using a multi-mass system model simulating a reinforced concrete (RC) chimney as a method which directly uses the obtained time-history waveforms.

In conventional evaluations of seismic capacity, the general practice was to use a simple technique[11] of estimating required strength from the assumed maximum surface response acceleration and natural period of chimney. This technique was derived experientially from the results of elastic response analysis using typical observed seismic waves (7 waveforms) and did not consider the effects of designated regions or earthquakes. On the other hand, use of time-history response analysis when evaluating the performance of chimneys with heights exceeding 60 m at the time of new construction has been legally required since 2007.

Therefore, an elasto-plastic time-history response analysis was carried out using a typical observed seismic wave (El Centro wave) and the seismic wave of scenario earthquake (scenario wave), and the results were compared with the strength requirement given by the guidelines for existing RC chimneys.

The chimney was assumed to be a nonlinear shear bending beam model comprising 12 mass points with a fixed foundation. The primary natural period of this chimney for initial stiffness is 1.57 s. Based on the method presented in Design Guidelines for Chimney Construction[12)], the skeleton curve of the restoring force characteristics with respect to bending was modeled by a tri-linear curve represented by 3 points, these being the cracking point of the concrete M_c, the yield strength of the outermost edge reinforcing steel on the tension side M_y, and the ultimate point due to compressive failure of the concrete on the compressive side M_u.

As results of the elasto-plastic response analysis for the El Centro wave and the scenario wave, **Fig. 11** shows a comparison of the maximum bending moment at each level of the chimney. The same figure also shows the required bending strength estimated based on the existing guidelines for RC chimney construction.

In this calculation example, the bending moments generated by the El Centro wave and scenario wave are smaller than the required bending strength under the guidelines for existing RC chimneys. Of course, the results will differ depending on the structural characteristics or the input seismic wave. However, under these conditions, the safety factor (=(strength capacity) / (required strength)) can be overestimated by the conventional method. Furthermore, in lower sections with heights of less than 80 m, the bending moment generated by the scenario wave (181 Gal (=1.81 m/s^2)) is approximately 1.5 times larger than that generated by the El Centro wave (342 Gal). Thus, not only the maximum response acceleration at the surface, but also differences in frequency characteristics, have a remarkable influence on response.

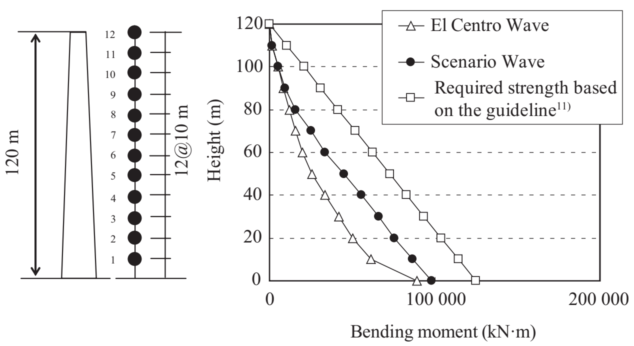

Fig. 11 Effects of different seismic wave on the response

For a final decision as to whether reinforcement (seismic retrofitting) is necessary or not, a judgment based on the results of a degradation study is necessary. However, this example confirmed that the safety factor can be evaluated correctly, and theoretical grounds for rational capital investment can be obtained, by a dynamic analysis using scenario ground motion.

5.2 Setting of Response Spectrum for Standard Design

Dynamic analysis using direct modeling of structures, as described above, is used in seismic study of critical structures and structures with special forms, such as blast furnaces, steel towers, quay walls, gas pipeline supports, and the like.

However, as a method of evaluating the seismic capacity of neatly-shaped low- and medium-rise structures and equipment and energy system structures using mainly static analysis, the design seismic coefficient estimated from response spectra corresponding to the natural period is frequently used. This simple evaluation technique is also effective in the primary screening stage in a steel works, which contains a large number of structures.

Therefore, as response spectra for use in simple static evaluations, the authors attempted to establish a response spectrum for standard design based on the scenario ground motion in each object zone.

First, the distribution frequency of maximum surface acceleration is prepared for the total area of the object zones calculated by the strong motion prediction method, and effective data for considering their variance is extracted. Next, a structural seismic response analysis for 1 mass system is performed using the surface acceleration response waveforms of the extracted data, and the envelope of the spectra curve is obtained by superposing all the obtained acceleration response spectra. In this process, the above-mentioned analysis of multiple expected earthquakes with different predominant periods is performed as far as possible, as frequency characteristics will differ depending on the scenario ground motion. Based on these envelopes, a result which has been smoothed in consideration of consistency with various standards was selected as the response spectrum for standard design.

An example of a response spectrum for standard

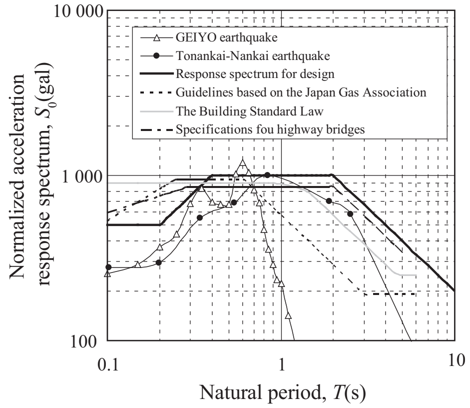

Fig. 12 Example of response spectrum for standard design

design is shown in **Fig. 12**, together with various standards. In this example, the maximum response velocity is set at 1 000 Gal, which is equivalent to an extremely rare major earthquake (C_0=1.0) in the Building Standard Law. On the long period side, this was decreased corresponding to the period in the range of T≥2 s so as to be above the envelope of the expected Tonankai-Nankai earthquake. The slope of this decrease conformed to Level 2 seismic motion, Type I (marine type) in the Specifications for Highway Bridges. On the other hand, on the short period side, the maximum response velocity was decreased in conformance with the envelope of an expected Geiyo earthquake, which is predominant in the range of T≤0.4s. However, as the lower limit, 500 Gal (T=0.1s) was adopted. This is equivalent to a Level 2 earthquake in the Guidelines based on the Japan Gas Association[13].

Response exceeding the set response spectrum for standard design appears partially in the vicinity of T=0.6s. Therefore, for structures with natural periods around this value, a dynamic analysis was used in combination with the method described above, based on individual checks of the ground characteristics at installation locations.

Selection of equipment and structures which required detailed study and setting of priority rankings are performed by a simple static evaluation using the response spectrum for standard design obtained in this manner, thereby improving the efficiency of evaluations of seismic capacity for diverse types of structures.

5.3 Application of Scenario Ground Motion to I_s

According to Notifications No. 184 and 185 of the Ministry of Land, Infrastructure, Transport and Tourism in 2006 based on the enactment of the Law for Promotion of Seismic Retrofitting of Buildings, which was adopted in light of the 1995 Hyogo-ken Nanbu earthquake, evaluations by the required seismic capacity index I_s can be used in the method of evaluation for seismic capacity. According to the Standard for Seismic Evaluation[14] of existing reinforced concrete buildings, the required seismic capacity index I_{so} can be expressed using the vibration characteristic coefficient R_t shown in Eq. (7) in evaluations using the value of I_s shown in Eq. (4), and when assuming neatly-shaped low- and medium-rise buildings, in correspondence with the current New Aseismic Design Code in Eqs. (5) and (6).

$$I_s \geq I_{so} = E_s \cdot Z \cdot G \cdot U \quad \cdots\cdots (4)$$

$$Q_{un} \geq D_s \cdot F_{es} \cdot Q_{ud} \quad \cdots\cdots (5)$$

$$Q_{ud} = Z \cdot R_t \cdot A_i \cdot C_0 \cdot W \quad \cdots\cdots (6)$$

$$I_s \geq I_{so} = 0.6 \cdot Z \cdot R_t \quad \cdots\cdots (7)$$

where, E_s: Basic index for evaluation of seismic capacity
Z: Seismic zoning index
G: Ground index
U: Use index
Q_{un}: Horizontal strength capacity required
Q_{ud}: Horizontal force during earthquake
D_s: Structural characteristics coefficient
F_{es}: Shape characteristic factor
A_i: Height distribution of story shear coefficient

The vibration characteristic coefficient R_t was specified under Notification No. 1793, Article 2 of the Ministry of Construction (1980). However, a provision allows use of a reduced numerical value based on special surveys or research (limited to 3/4 of the numerical value specified by the Notification). Since R_t is equivalent to the standardized response spectrum for design, it is possible to set the value of I_{so} for frequency dependence relative to scenario ground motion by regarding the aforementioned response spectrum (spectral shape) for standard design as R_t.

At JFE Steel's West Japan Works, which will be strongly affected by subduction type earthquakes, a seismic determination for buildings was made using the I_{so} value based on scenario ground motion. In comparison with determinations by the I_{so} value (=0.6× (seismic zoning factor 0.9)) which is set uniformly independent of local conditions, the results confirmed that the number of buildings which do not satisfy I_{so} (have inadequate seismic performance and are judged to require immediate seismic retrofitting) can be reduced by approximately 15%.

6. Conclusion

This paper described a method of estimating recent strong ground motion which accurately reflects the local strata of steel works. An evaluation of seismic capacity which incorporates response characteristics based on the obtained scenario ground motion in various design standards was proposed, and it was shown that diverse structures can be evaluated efficiently and rationally using this method. At present, evaluations of seismic capacity of individual structures based on this method are progressing steadily in cooperation with the departments responsible for the structures, and implementation of concrete seismic retrofitting measures has begun. As the earthquake damage prediction technology described herein can also be applied widely outside of this company, the JFE Group has created a system which is capable of responding to the needs of clients with other types of large-scale plants such as energy facilities.

JFE Steel is committed to making every possible effort to contribute to the business continuity plans (BCP) of its clients by maintaining a stable supply of products. To this end, we intend to further improve the accuracy of earthquake damage prediction and ensure the safety and security of steel works.

The computational program used in this method, and guidance in its method of use, were provided by Atsushi Nozu, Head of Group, Engineering Seismology Group, Port and Airport Research Institute. For seismic ground motion observation records, Strong-Motion Earthquake Records in Japanese Ports (National Institute for Land and Infrastructure Management, Ministry of Land, Infrastructure, Transport and Tourism, etc.) and the Kyoshin Network (K-net: Strong Motion Network; National Research Institute for Earth Science and Disaster Prevention) were used.

References

1) Ministry of Education, Culture, Sports, Science and Technology, The Headquarters for Earthquake Research Promotion, Earthquake Research Committee. National Seismic Hazard Maps for Japan. 2005.
2) Japan Road Association. Specifications for Highway Bridges, PART V Seismic Design. 2002-03
3) Annaka, Tadashi et al. Proposal of an Estimation Formula of the Largest Earth Motion and Response Spectrum using the record of the 87 type strong motion seismometer of Meteorological Agency, Japan Society of Civil Engineers. Journal of Earthquake Engineering. 1997, vol. 24, p. 161–164.
4) The Ports & Harbours Association of Japan. Technical Standards and Commentaries for Port and Harbour Facilities in Japan. 2007-07, vol. 1, 2.
5) Kowada, Akira et al. Evaluation of Horizontal and Vertical Strong Ground Motions using Empirical Site-Specific Amplification and Phase Characteristics. Journal of Structural and Construction Engineering, Architectural Institute of Japan. 1998-12, vol. 514, p. 97–104.
6) Cabinet Office, Government of Japan, Central Disaster Management Council. Shuto Chokka Jishin Taisaku Senmon Chosakai. 2004-11. vol. 12, no. 2-2. (Japanese).
7) Nozu, Atsushi; Nagao, Takashi. Site Amplification Factors for Strong-Motion Sites in Japan Based on Spectral Inversion Technique, Technical note of the Port and Airport Research Institute. 2005-12, no. 1112.
8) National Research Institute for Earth Science and Disaster Prevention. Kyoshin-Network (K-NET).
9) Iai, S.; Matsunaga, Y.; Kameoka, T. Strain Space Plasticity Model for Cyclic Mobility. Report of the Port and Harbour Research Institute. 1990, vol. 29, no. 4, p. 27–56.
10) Iai, S.; Kameoka, T. Finite element analysis of earthquake induced damage to anchored sheet pile quay walls. Soils and Foundations. 1993, vol. 33, no. 1, p. 71–91.
11) Japan Building Disaster Prevention Association. Kizon RC Zou Entotsu no Taikyu · Taishin Shindan Shishin. 1981. (Japanese).
12) Architectural Institute of Japan. Entotsu Kozou Sekkei Shishin. 2007-11. (Japanese).
13) Japan Gas Association. Seizou Setsubi Tou Taishin Sekkei Shishin Kaiteiban. 2001-08. (Japanese).
14) Japan Building Disaster Prevention Association. Kizon Tekkin Concrete Zou Kenchikubutsu no Taishin Shindan Kijun · Dou Kaisetsu. 2001. (Japanese).